



Pacific Northwest
NATIONAL LABORATORY

Proudly Operated by Battelle Since 1965

Detecting the Extent of Eutectoid Transformation in U-10Mo

August 2016

A Devaraj
S. Jana
C Mcinnis
NJ Lombardo

VV Joshi
L. Sweet
S Manandhar
CA Lavender

DISCLAIMER

This report was prepared as an account of work sponsored by an agency of the United States Government. Neither the United States Government nor any agency thereof, nor Battelle Memorial Institute, nor any of their employees, makes **any warranty, express or implied, or assumes any legal liability or responsibility for the accuracy, completeness, or usefulness of any information, apparatus, product, or process disclosed, or represents that its use would not infringe privately owned rights.** Reference herein to any specific commercial product, process, or service by trade name, trademark, manufacturer, or otherwise does not necessarily constitute or imply its endorsement, recommendation, or favoring by the United States Government or any agency thereof, or Battelle Memorial Institute. The views and opinions of authors expressed herein do not necessarily state or reflect those of the United States Government or any agency thereof.

PACIFIC NORTHWEST NATIONAL LABORATORY
operated by
BATTELLE
for the
UNITED STATES DEPARTMENT OF ENERGY
under Contract DE-AC05-76RL01830

Printed in the United States of America

Available to DOE and DOE contractors from the
Office of Scientific and Technical Information,
P.O. Box 62, Oak Ridge, TN 37831-0062;
ph: (865) 576-8401
fax: (865) 576-5728
email: reports@adonis.osti.gov

Available to the public from the National Technical Information Service
5301 Shawnee Rd., Alexandria, VA 22312
ph: (800) 553-NTIS (6847)
email: orders@ntis.gov <<http://www.ntis.gov/about/form.aspx>>
Online ordering: <http://www.ntis.gov>



This document was printed on recycled paper.

(8/2010)

Detecting the Extent of Eutectoid Transformation in U-10Mo

A Devaraj
S. Jana
C Mcinnis
NJ Lombardo

VV Joshi
L Sweet
S Manandhar
CA Lavender

August 2016

Prepared for
the U.S. Department of Energy
under Contract DE-AC05-76RL01830

Pacific Northwest National Laboratory
Richland, Washington 99352

Executive Summary

During eutectoid transformation of U-10Mo alloy, uniform metastable γ UMo phase is expected to transform to a mixture of α -U and γ' -U₂Mo phase. The presence of transformation products in final U-10Mo fuel, especially the α phase is considered detrimental for fuel irradiation performance, so it is critical to accurately evaluate the extent of transformation in the final U-10Mo alloy. This phase transformation can cause a volume change that induces a density change in final alloy. To understand this density and volume change, we developed a theoretical model to calculate the volume expansion and resultant density change of U-10Mo alloy as a function of the extent of eutectoid transformation. Based on the theoretically calculated density change for 0 to 100% transformation, we conclude that an experimental density measurement system will be challenging to employ to reliably detect and quantify the extent of transformation.

Subsequently, to assess the ability of various methods to detect the transformation in U-10Mo, we annealed U-10Mo alloy samples at 500°C for various times to achieve in low, medium, and high extent of transformation. After the heat treatment at 500°C, the samples were metallographically polished and subjected to optical microscopy and x-ray diffraction (XRD) methods. Based on our assessment, optical microscopy and image processing can be used to determine the transformed area fraction, which can then be correlated with the α phase volume fraction measured by XRD analysis. XRD analysis of U-10Mo aged at 500°C detected only α phase and no γ' was detected. To further validate the XRD results, atom probe tomography (APT) was used to understand the composition of transformed regions in U-10Mo alloys aged at 500°C for 10 hours. Based on the APT results, the lamellar transformation product was found to comprise α phase with close to 0 at% Mo and γ phase with 28–32 at% Mo, and the Mo concentration was highest at the α/γ interface.

Acronyms and Abbreviations

°C	degrees Celsius
APT	atom probe tomography
BCC	body-centered cubic
C	carbon
cm ³	cubic centimeter(s)
EDS	energy-dispersive x-ray spectroscopy
g	gram(s)
Mo	molybdenum
PNNL	Pacific Northwest National Laboratory
SEM	scanning electron microscopy
U	uranium
U-10Mo	uranium alloyed with 10 weight percent molybdenum
UMo	body-centered cubic γ -UMo
wt%	weight percent
XRD	x-ray diffraction

Contents

Executive Summary	iii
Acronyms and Abbreviations	v
1.0 Introduction	1
2.0 Determination of the Theoretical Volume Fractions of α -U and γ' -U ₂ Mo Phases as a Function of the Percentage Transformed	2
3.0 Estimating the Density and Volume Expansion as a Function of Percent Transformation	4
3.1 Motivation for Calculation of Effective Density	4
3.2 Calculation of Density of Parent (γ) and Product Phases ($\alpha + \gamma'$)	4
3.3 Estimating Effective Density of Final Alloy	5
3.4 Volume Expansion of the Final Alloy as a Function of Extent of Transformation	6
4.0 Microscopy and XRD Based Methods	7
5.0 Conclusions	10
6.0 Recommendations	10
7.0 References	10

Figures

Figure 1.	a) The U-Mo phase diagram and the formation of various phases; and b) the U-10Mo time-temperature transformation curve (Mcgeary et. al.)	1
Figure 2.	(a) Backscattered SEM image of 500°C-30 hour aged U-10Mo alloy showing the lamellar eutectoid transformation; (b) schematic showing the decomposition of γ -UMo to α -U and γ' -U ₂ Mo phases. The arrows indicate the parent γ -UMo region and transformed region.	4
Figure 3.	Percent transformed vs. effective density of final U-10Mo alloy.....	5
Figure 4.	Volume expansion of the final alloy vs. the percent transformed.	6
Figure 5.	The 10X optical microscopy image and corresponding XRD spectra along with the measured crystalline size, strain, and α -U volume fraction for DUMo 242 (a, b), DUMo 240 (c, d), and DUMo 239 (e, f), indicating the increasing degree of transformation; and (g) the graphical representation of converting the XRD-measured α volume fraction to total area transformed.	8
Figure 6.	(a) SEM image of transformed region in DUMo 562 from where atom probe samples were prepared; (b) the atom probe result showing the α -U region in purple and the Mo-rich lamellar region in red; and (c) the composition partitioning between α -U and Mo-rich γ -UMo showing Mo concentration between 32.2 and 28.2 at% as a function of the distance from the α/γ interface going into γ region.	9

Tables

Table 1.	Theoretically expected equilibrium volume fractions of γ , α , and γ' for 0 to 15% transformation. In accordance with the current U-10Mo fuel specification up to 10% transformation is considered acceptable. Hence, this table will serve as the detailed reference within and just above the specification limit for the maximum extent of transformation allowed in the final U-10Mo alloy fuel product.	2
Table 2.	Theoretically estimated volume fraction of γ -U10Mo, α -U and γ' -U ₂ Mo as a function of percent transformed obtained by the lever rule, based estimation of a 0.35166 volume fraction of α phase and a 0.64834 volume fraction of γ' phase in the transformation product.	3
Table 3.	The composition of both transformation product phases as measured by APT 6 nm away from the interface.....	9

1.0 Introduction

The Fuel Fabrication Capability pillar of the Reactor Conversion program is focused on developing a streamlined fuel manufacturing method. Doing so will require increased understanding of the effects of processing conditions on the final fuel microstructure. During the entire process flow—from casting to final fuel form—uranium (U) alloyed with 10 wt% molybdenum (U-10Mo) is subjected to different time-temperature histories. Some of these temperatures are very close to the eutectoid transformation temperature of the U-10Mo alloy. Hence, the temperatures are expected to result in different extents of transformation at which the uniform parent γ U-Mo phase is expected to transform to a lamellar mixture of α -U and γ' -U₂Mo phases, as shown in Figure 1a and 1b. It is important to detect such eutectoid transformations and estimate their extents of because the presence of α -U is detrimental to the mechanical stability of the alloy owing to its anisotropic thermal expansion properties.

At Pacific Northwest National Laboratory (PNNL) various methods are used to detect this transformation. First, microscopy of metallographically polished specimens by either optical microscopy or scanning electron microscopy (SEM) imaging is used. This method can identify the transformed regions and measure an area fraction that is usable as a measure of the percent transformed, but it is fairly time consuming. Another method, x-ray diffraction (XRD), has a faster throughput, but its detection limit and ability to detect both transformation products are of concern. The third method of identifying and measuring the extent of transformation relies on a change in the final volume of the alloy due to the transformation affecting the final density of the alloy product. If significant changes are expected in density as a result of eutectoid transformation, a simple density measurement system at various stages of alloy processing could be used to measure the extent of transformation. Using such a system would reduce the time and effort required to estimate the extent of transformation in the U-10Mo fuel. At present, concise descriptions of each of these three methods and their benefits and drawbacks are not clearly documented in the U-10Mo literature. This report focuses on filling this need.

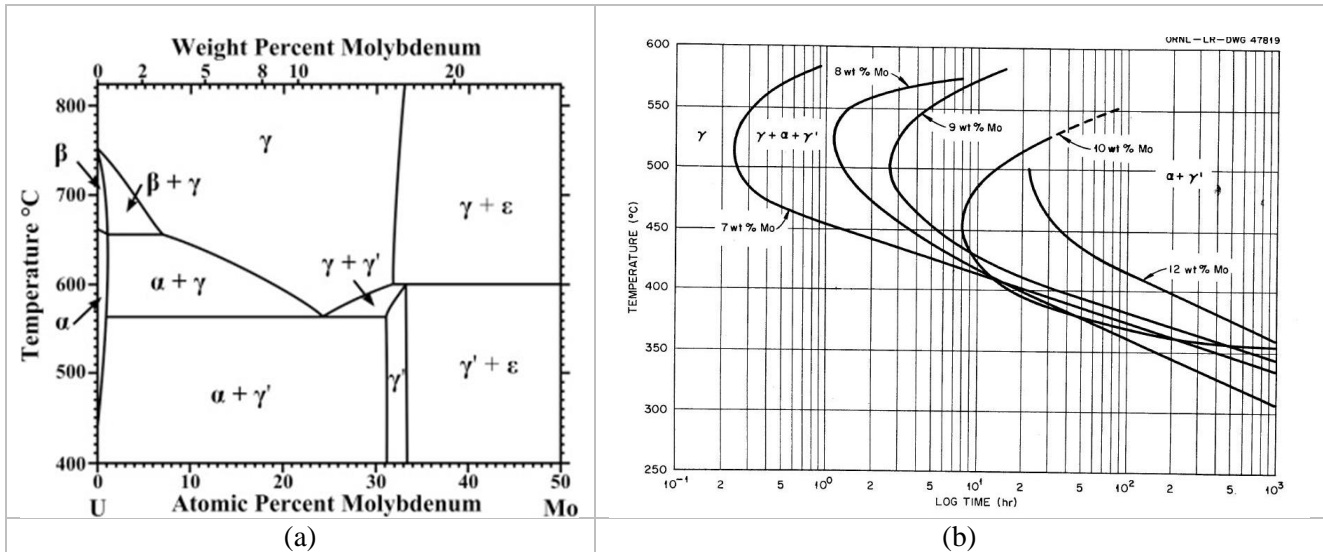


Figure 1. a) The U-Mo phase diagram and the formation of various phases; and b) the U-10Mo time-temperature transformation curve (Mcgeary et. al. 1955)

This report is expected to serve as the reference for the procedures used to evaluate the extent of transformation in U-10Mo alloy and for the volume expansion and density change of the final U-10Mo alloy as a function of the extent of transformation. The report initially describes the fraction of transformation of α -U and γ' -U₂Mo phases as a function of the percent transformed based on the theoretical calculations (Section 2.0). The ensuing sections then delve into the techniques used to determine the exact volume fraction of transformation.

2.0 Determination of the Theoretical Volume Fractions of α -U and γ' -U₂Mo Phases as a Function of the Percentage Transformed

Based on the U-Mo phase diagram (Figure 1a), the lever rule can be applied to obtain volume fractions of α and γ' phases at different transformation temperatures. Assuming there is no Mo solubility in α -U and 33.33 at% γ' -U₂Mo as products and an alloy composition of 10 wt% Mo, which is equivalent to 21.61124 at%, the α and γ' phase volume fractions in the transformation product can be calculated as follows:

$$\text{Volume fraction of } \alpha = \frac{(33.3333 - 21.61124)}{(33.3333 - 0)} = 0.35166$$

$$\text{Volume fraction of } U_2Mo = \frac{(21.61124 - 0)}{(33.3333 - 0)} = 0.64834$$

Hence, the percent of transformation can be decomposed to the corresponding α and γ' volume fractions expected. The table for percent of transformation vs. α and γ' volume fractions is given below for 0-15% transformation with 1% increments (Table 1) and for 0–100% transformation with 5% increments (Table 2), both of which can serve as look-up tables for validating other measurements like the XRD-measured volume fraction of α . Note that the volume fraction of γ' can be calculated by multiplying the volume fraction of α by a multiplication factor of 1.84365 in accordance with the lever rule.

Note that this look-up table is only valid for U-10 wt% Mo, assuming transformation produces α -U with no Mo and γ' -U₂Mo with exact stoichiometry. Based on the phase diagram there can be some limited solubility of Mo in α -U, and a finite extent of off-stoichiometry is sustainable in U₂Mo because it is not a line compound in the phase diagram. Also, eutectoid reaction is known to sometimes also produce a mixture of α -U and γ -UMo rather than the equilibrium product of α -U and γ' -U₂Mo (Neogy et al. 2012, 2015). Finally, it should be noted that formation of such non-equilibrium transformation products can also change the final phase fractions observed during transformation.

Table 1. Theoretically expected equilibrium volume fractions of γ , α , and γ' for 0 to 15% transformation. In accordance with the current U-10Mo fuel specification up to 10% transformation is considered acceptable. Hence, this table will serve as the detailed reference within and just above the specification limit for the maximum extent of transformation allowed in the final U-10Mo alloy fuel product.

Percent Transformed	Volume Fraction of γ U-10Mo	Volume Fraction of α -U	Volume Fraction of U ₂ Mo (γ')
0	100	0.00	0.00
1	99	0.35	0.65
2	98	0.70	1.30
3	97	1.05	1.95
4	96	1.41	2.59

Table 1. (contd)

Percent Transformed	Volume Fraction of γ U-10Mo	Volume Fraction of α -U	Volume Fraction of U ₂ Mo (γ')
---------------------	------------------------------------	--------------------------------	--

5	95	1.76	3.24
6	94	2.11	3.89
7	93	2.46	4.54
8	92	2.81	5.19
9	91	3.16	5.84
10	90	3.52	6.48
11	89	3.87	7.13
12	88	4.22	7.78
13	87	4.57	8.43
14	86	4.92	9.08
15	85	5.27	9.73

Table 2. Theoretically estimated volume fraction of γ -U10Mo, α -U and γ' -U₂Mo as a function of percent transformed obtained by the lever rule, based estimation of a 0.35166 volume fraction of α phase and a 0.64834 volume fraction of γ' phase in the transformation product.

Percent Transformed	Volume Fraction of γ U-10Mo	Volume Fraction of α -U	Volume Fraction of U ₂ Mo (γ')
0	100	0.00	0.00
5	95	1.76	3.24
10	90	3.52	6.48
15	85	5.27	9.73
20	80	7.03	12.97
25	75	8.79	16.21
30	70	10.55	19.45
35	65	12.31	22.69
40	60	14.07	25.93
45	55	15.82	29.18
50	50	17.58	32.42
55	45	19.34	35.66
60	40	21.10	38.90
65	35	22.86	42.14
70	30	24.62	45.38
75	25	26.37	48.63
80	20	28.13	51.87
85	15	29.89	55.11
90	10	31.65	58.35
95	5	33.41	61.59
100	0	35.17	64.83

The following sections describe the various techniques that can be used to estimate the volume fraction of the transformation.

3.0 Estimating the Density and Volume Expansion as a Function of Percent Transformation

3.1 Motivation for Calculation of Effective Density

A typical backscattered SEM image of a partially transformed microstructure of U-10Mo is given in Figure 2(a). The crystallographic change associated with this transformation is shown schematically in Figure 2(b). At present there is no clear mathematic model linking the extent of transformation with the overall volume expansion of the final alloy or effective density. To address this gap, we developed a model to calculate both the effective density and the volume expansion of the U-10Mo final alloy as a function of the extent of transformation.

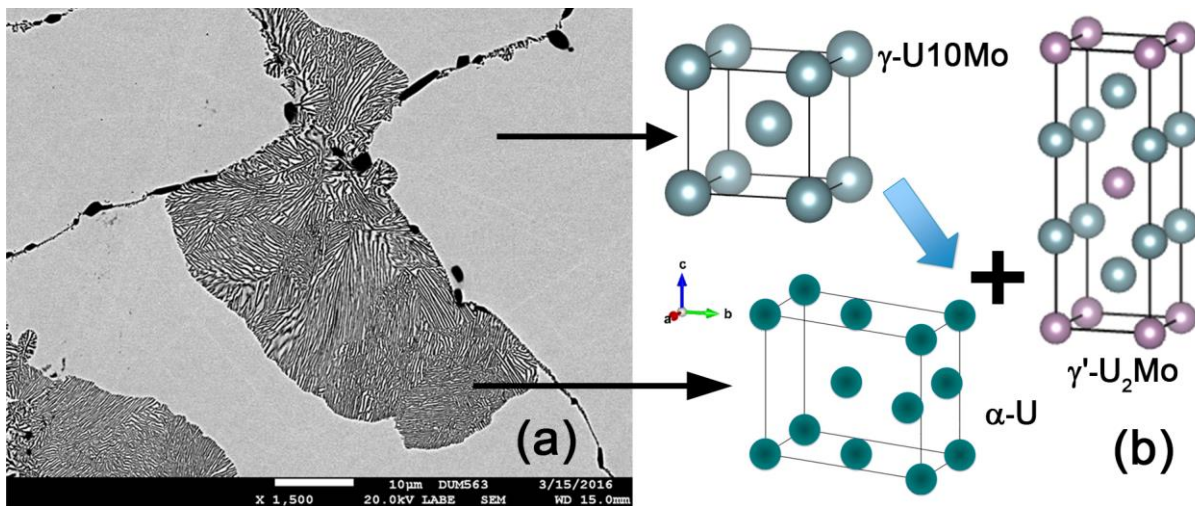


Figure 2. (a) Backscattered SEM image of 500°C-30 hour aged U-10Mo alloy showing the lamellar eutectoid transformation; (b) schematic showing the decomposition of γ -UMo to α -U and γ' -U₂Mo phases. The arrows indicate the parent γ -UMo region and transformed region.

Using the volume fraction of different phases in the transformation product estimated in Section 2.0, the effective density can be calculated as a function of the extent of transformation in two steps: first by calculating effective density of parent and product phases, and then by using the rule of mixture to estimate the effective density of final alloy.

3.2 Calculation of Density of Parent (γ) and Product Phases ($\alpha + \gamma'$)

The densities of parent γ -UMo and transformation product phases α -U and γ' -U₂Mo phases were calculated based on a single unit cell.

From the literature, γ -UMo is known to have a body-centered cubic (BCC) structure. The density of γ -UMo phase with 19.75 wt% U²³⁵ enrichment was estimated in a past report to be 17.33187 g/cm³ (Devaraj 2016).

α -U is assumed to have no solubility of Mo and it is known to have a face-centered orthorhombic unit cell with 4 atoms per unit cell and lattice parameters of $a = 2.8537 \text{ \AA}$, $b = 5.8695 \text{ \AA}$ and $c = 4.9548 \text{ \AA}$ (Barrett et.al. 1963). Based on this, the density of α -U was estimated to be 19.00443 g/cm³.

U₂Mo is assumed to have a body-centered tetragonal structure similar to MoSi₂ with lattice parameters of a = 3.427 Å and c = 9.834 Å and with 6 atoms per unit cell (4 U and 2 Mo atoms) (Haltzman 1957). Based on this, the density of U₂Mo was estimated to be 16.41513 g/cm³.

3.3 Estimating Effective Density of Final Alloy

Once the final volume fraction of γ -U10Mo, α -U and γ' -U₂Mo as a function of the percent transformed is obtained (as given in Section 2.0), the individual volume fraction of phases can be used to calculate the effective density of the final alloy based on the formula

$$\begin{aligned} \text{Effective density of final alloy} \\ = \text{Volume fraction of } \gamma - \text{U10Mo} \times \text{density of } \gamma - \text{U10Mo} + \text{Volume fraction of } \alpha - \text{U} \\ \times \text{density of } \alpha - \text{U} + \text{Volume fraction of } \gamma' - \text{U2Mo} \times \text{Density of } \gamma' - \text{U2Mo} \end{aligned}$$

The calculated density vs. percent of transformation is given in Figure 3.

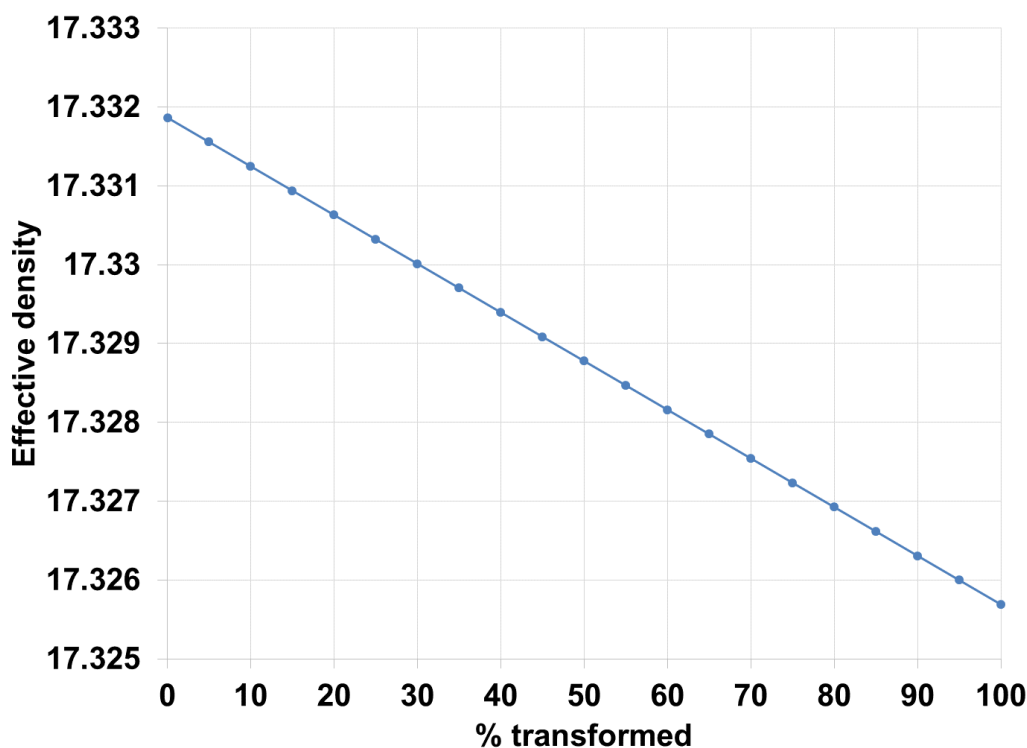


Figure 3. Percent transformed vs. effective density of final U-10Mo alloy.

From the graph, it can be seen that the density only changes from the second decimal space onwards when going from 0 to 100% transformation, indicating the need for a precise density measurement system to estimate the extent of transformation (Prabhakaran 2016; Devaraj 2015).

3.4 Volume Expansion of the Final Alloy as a Function of Extent of Transformation

Once we have the effective density of the final alloy, the volume expansion can be estimated by taking an inverse of density of the final alloy at each percent transformation value, and using the equation below.

Volume expansion as a function of % transformation

$$= \frac{\left(\frac{1}{\text{density of final alloy with } x\% \text{ transformation}} \right) - \left(\frac{1}{\text{density of alloy with } 100\% \gamma} \right)}{\left(\frac{1}{\text{density of alloy with } 100\% \gamma} \right)}$$

Similar to the previous results, from the graph in Figure 4, it can be seen that there is only very minimal volume expansion even up to 100% transformation in the U-10Mo alloy.

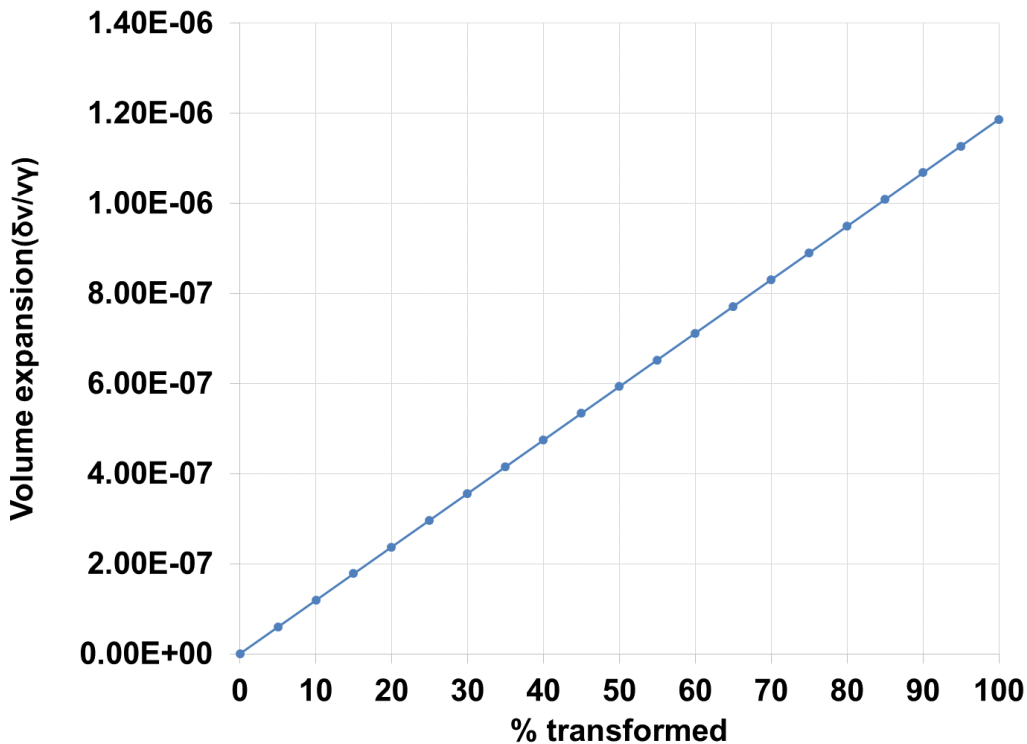


Figure 4. Volume expansion of the final alloy vs. the percent transformed.

Thus the measurement of density and volume alike will require precise measurement techniques to monitor any phase transformations, and will be challenging while implementing the same on the shop floor to determine the phase transformation.

Supplementary Information: The worksheet with the entire calculation are provided in the accompanying Excel file named “Transformation_Effective density_5July2016.xlsx.”

4.0 Microscopy and XRD Based Methods

The U-10Mo alloy is ideally expected to be predominantly BCC-structured γ -UMo, hereafter called UMo phase (Burkes et al. 2009, 2010; Joshi et al. 2015a, 2015b). However, during the extensive U-10Mo fuel processing—from as-cast ingots to fuel plate—and especially during some steps like the hot isostatic pressing process, the U-10Mo alloy can be subjected to temperatures very close to the eutectoid transformation temperature, which can induce a eutectoid transformation of the γ -UMo phase, thereby forming a lamellar mixture of α -U and γ' -U₂Mo phases. Metallographic polishing of transformed samples followed by optical or electron microscopy can reveal the transformation in U-10Mo alloys based on the contrast between images.

For the current work, XRD analysis was conducted in a Rigaku Ultima IV equipped with a monochromated Cu K- α x-ray source and a linear position-sensitive silicon strip detector. In general, diffraction data were collected between 25° and 120° 2 θ in 0.001° increments at a scan rate of 0.5°/min. Full pattern Rietveld refinement was performed using TOPAS v4 (Bruker) to obtain the relative weight percent of the phases identified in each pattern. National Institute of Standards and Technology-certified reference material 640d was used as an external standard to determine instrument alignment and peak shape profile parameters. The crystallite size reported was from the peak integral breadth of the Lorentzian type convolution as implemented in TOPAS v4 and described elsewhere (Balzar 1999). The unit cell parameter of γ -U metal was refined for each pattern collected. The details of the metallographic preparation can be found in a previous report (Prabhakaran et al. 2015).

Microstructural characterization was performed using an optical microscope as well as a JEOL JSM-7600F SEM equipped with an Oxford Instruments X-Max 80 energy-dispersive x-ray spectroscopy (EDS) detector. The EDS analysis was performed using INCA Microanalysis Suite software, version 4.15.

To quantify the amount of transformation, image analysis was conducted using the ImageJ software. In ImageJ, a gray-scale image was first opened, and the length of the micron marker was recorded using the “set scale” option available under the “Analyze” tab. The gray-scale image was then converted into a black and white image by thresholding the image. The “Threshold” option available under the “Image” tab was selected, then the “Adjust” option. The degree of thresholding depends on user preference; i.e., what are the features that the user wants to quantify. For example, a low level of thresholding helps determine the volume fraction of second phase fine particles, while a higher degree of thresholding helps in identify the volume fraction of eutectoid transformation products.

Figure 5 presents the results of optical microscopy results from the least transformed microstructure to almost completely transformed microstructures, all taken at 10X magnification. The dark contrast is specifically arising from the transformed regions. In Figure 5(a) the transformed regions are predominantly restricted to grain boundary areas, whereas in Figure 5(c) many grains are entirely transformed. The estimate of the transformed microstructure area fractions measured based on image processing of optical micrograph images given in Figure 5(a), (c) and (e) are 12.8%, 20% and 57.7%, respectively. XRD results of samples in Figure 5(a), (c) and (e) given in (b), (d) and (f) detected only 1.19%, 3.1 %, and 17% α -U phase, while detecting no γ' phase. In accordance with the lever rule, based on calculations given in Table 1 and Table 2, the volume fraction of γ' can be calculated by multiplying the α volume fraction by 1.84. Assuming a similar relationship in the experimentally measured volume fractions of phases, the XRD-measured volume fraction of α phase can be multiplied by 1.84 to obtain the γ' volume fraction. The summation of the two should provide the area fraction of transformation calculated based on XRD. In Figure 5(g) the calculated extent of the area of transformation based on XRD is plotted against the optically measured area fraction results for all three extents of transformation. From Figure 5, it is clear that the transformation area calculated by XRD under-estimates the total transformation extent.

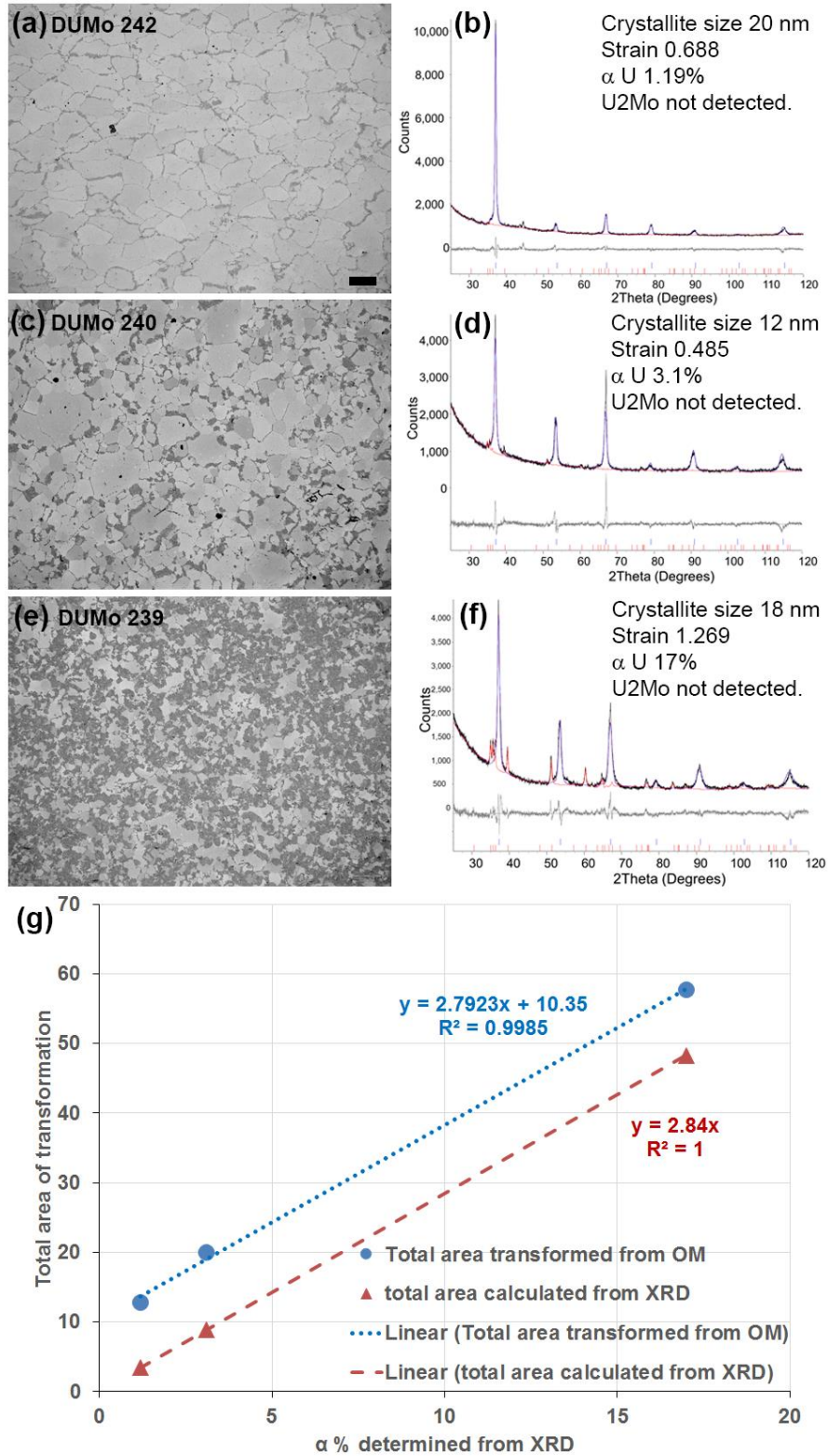


Figure 5. The 10X optical microscopy image and corresponding XRD spectra along with the measured crystalline size, strain, and α -U volume fraction for DUMo 242 (a, b), DUMo 240 (c, d), and DUMo 239 (e, f), indicating the increasing degree of transformation; and (g) the graphical representation of converting the XRD-measured α volume fraction to total area transformed.

The composition of long lamellar regions in DUMo 562 (as-cast followed by homogenization at 900°C for 48 hours and aging at 500°C for 10 hours) was analyzed using atom probe tomography (APT). The SEM image of the transformed region selected to prepare the APT specimens is shown in Figure 6(a). The APT result highlighting the α -U-rich and Mo-rich γ -UMo regions within the transformed region is given in Figure 6(b). The composition partitioning between both phases is given as a function of the distance from the interface in Figure 6(c). The composition of α and γ phases in the transformation product as measured by APT is given in Table 3, in which it can be seen that the composition of the Mo-rich regions has not yet reached the 33.33 at% required to be a stable γ' -U₂Mo product. In addition to such regions additional transformation products of $\gamma + \gamma'$ in either long lamellar form or discontinuous short lamellas are also shown to exist in U-9Mo (Neogy et. al. 2012, Neogy et. al 2015). Such transformation products may also be present in U10Mo alloys aged at 500C. These non equilibrium transformation products can be the root cause of why XRD is unable to detect the presence of γ' -U₂Mo and only detects α -U in transformed U-10Mo alloys.

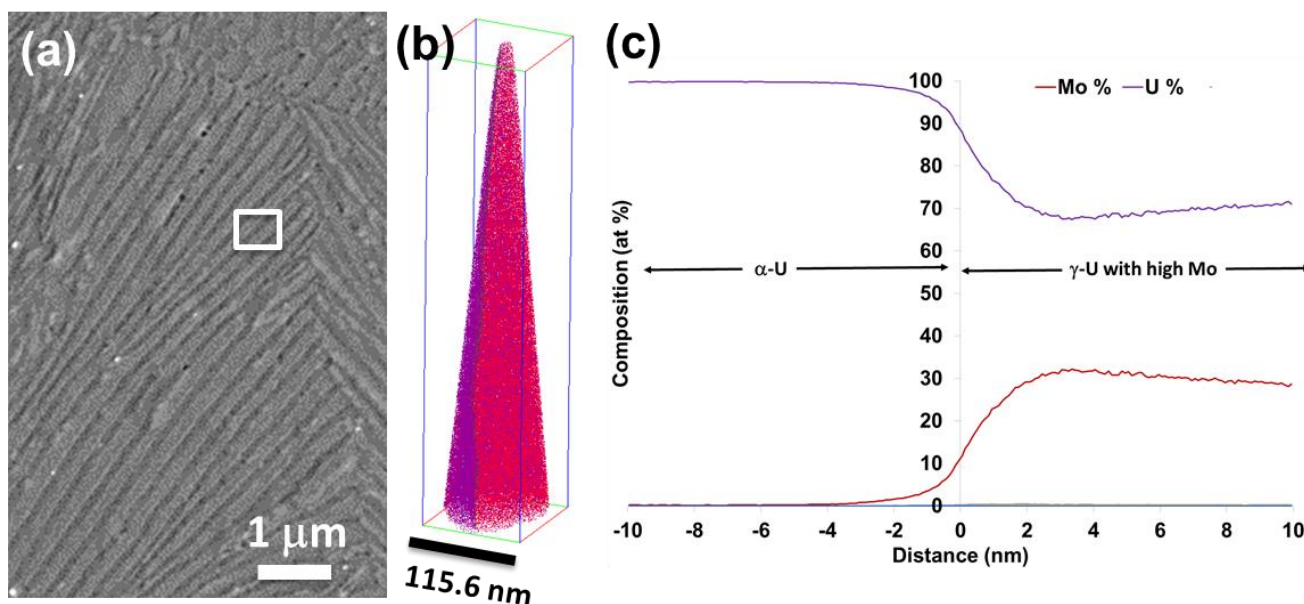


Figure 6. (a) SEM image of transformed region in DUMo 562 from where atom probe samples were prepared; (b) the atom probe result showing the α -U region in purple and the Mo-rich lamellar region in red; and (c) the composition partitioning between α -U and Mo-rich γ -UMo showing Mo concentration between 32.2 and 28.2 at% as a function of the distance from the α/γ interface going into γ region.

Table 3. The composition of both transformation product phases as measured by APT 6 nm away from the interface.

Phase ID	Mo %	U %	Al %	Si %	O %
α composition	0.196	99.776	0.001	0.025	0.001
γ composition	29.113	70.599	0.077	0.208	0.003

5.0 Conclusions

This report examined three approaches for determining the percent of transformation of U-10Mo alloys: density or volume expansion measurements, optical microscopy, and XRD. Our assessment of the three approaches derived the following outcomes:

- Theoretical lever rule-based calculations were developed to serve as a quick look-up tables of the expected volume fractions of α and γ' phases for various extents of percent transformation.
- Based on the theoretical calculations of expected density and volume expansion changes as a function of percent transformation, we conclude that a high-precision density measurement system will be needed to precisely evaluate the % transformation in U-10Mo alloys, especially below 15% transformation. The accuracy of the required measurements and the range of factors that can influence alloy density can make this approach very challenging to implement for accurately determining the % transformation of U-10Mo alloys.
- We demonstrated the use of optical microscopy and image analysis using Image J software to estimate the percent area of transformation in U-10Mo alloys aged at 500°C for various times with different extents of transformation.
- XRD only detected α and γ phases in U-10Mo alloys aged at 500°C for various times with no indication of γ' phase. In comparison with transformed area fraction measured by optical microscopy, the extent of transformation measured by XRD appeared be consistently and significantly under predicted.
- Based on APT analysis of the U-10Mo alloy aged at 500°C for 10 hours, the transformed regions predominantly consisted of α with almost no Mo and Mo-rich γ regions with less than 33 at% Mo. This can explain the inability of XRD to detect γ' phase in the 500°C aged U-10Mo alloy.

6.0 Recommendations

During the U-10Mo alloy manufacturing process the alloy can be subjected to a range of temperatures above and below the eutectoid transformation temperature near 500°C. Based on published literature, various transformation products are predicted as a function of the exact U-Mo alloy composition and transformation temperature. More experimental characterization work using optical microscopy, XRD, transmission electron microscopy, and APT are required to conclusively provide the feasibility to accurately measure the extent of transformation at other temperatures in addition to the 500°C annealing results given in this report. Also, extended annealing at each of the temperatures might lead to the formation of equilibrium transformation products, as predicted based on the phase diagram. Such long-time annealed samples also need to be analyzed using characterization methods to verify whether an improved match can be achieved between the theoretically predicted volume fraction of product phases and experimental measurements.

7.0 References

Balzar D. 1999. Voigt-function model in diffraction line broadening analysis. *Microstructure Analysis from Diffraction*, RL Snyder, HJ Bunge, and J Fiala (eds.), International Union of Crystallography.

Barrett CS, MH Mueller, RL Hitterman. 1963. "Crystal structure variations in Alpha Uranium at Low Temperatures" *Physical Review* 129 (2), 625-629.

Burkes D, R Prabhakaran, T Hartmann, J-F Jue, and F Rice. 2010. "Properties of DU-10 wt% Mo alloys subjected to various post-rolling heat treatments." *Nuclear Engineering and Design* 240:1332–1339.

Burkes D, T Hartmann, R Prabhakaran, and J-F Jue. 2009. Microstructural characteristics of DU-xMo alloys with x = 7-12 wt%." *Journal of Alloys and Compounds* 479:140–147.

E.K. Halteman EK. 1957. "The crystal structure of U₂Mo". *Acta Crystallographica* 10:166

Joshi V, E Nyberg, C Lavender, D Paxton, and D Burkes. 2015a. "Thermomechanical process optimization of U-10wt% Mo – Part 2: The effect of homogenization on the mechanical properties and microstructure." *Journal of Nuclear Materials* 465:710–718.

Joshi V, E Nyberg, C Lavender, D Paxton, H Garmestani, and D Burkes. 2015b. "Thermomechanical process optimization of U-10 wt% Mo – Part 1: High-temperature compressive properties and microstructure." *Journal of Nuclear Materials* 465:805–813.

Devaraj A., V Joshi, R Prabhakaran, SY Hu, E McGarrah, C Lavender 2016. "Theoretical Model for Volume Fraction of UC, 235U Enrichment, and Effective Density of Final U 10Mo Alloy" PNNL Report

R.K. McGeary (Ed.), Development and Properties of Uranium-Base Alloys Corrosion Resistant in High-Temperature Water, Pt. I., Alloys Without Protective Cladding, WAPD-127, 1955.

Neogy S, MT Saify, SK Jha, D Srivastava, MM Hussain, GK Dey, RP Singh 2012. "Microstructural study of gamma phase stability in U-9 wt.% Mo alloy." *Journal of Nuclear Materials* 422:77–85.

Neogy S, MT Saify, SK Jha, D Srivastava, GK Dey 2015. "Ageing characteristics of the metastable gamma phase in U-9 wt.% Mo alloy: experimental observations and thermodynamic validation" *Philosophical Magazine*, 95(26):2866–2884.

Prabhakaran R, VV Joshi, MA Rhodes, AL Schemer-Kohn, AD Guzman, and CA Lavender. 2016. U-10Mo Sample Preparation and Examination using Optical and Scanning Electron Microscopy . PNNL-25308, Pacific Northwest National Laboratory, Richland, WA.

Prabhakaran R, VV Joshi, A Devaraj, and CA Lavender. 2016 Procedure for U-Mo density measurement and porosity determination . *to be published*, Pacific Northwest National Laboratory, Richland, WA.



Pacific Northwest
NATIONAL LABORATORY

*Proudly Operated by **Battelle** Since 1965*

902 Battelle Boulevard
P.O. Box 999
Richland, WA 99352
1-888-375-PNNL (7665)

U.S. DEPARTMENT OF
ENERGY

www.pnnl.gov